Topological phases and phase transitions in magnets and ice

Keesman, R.

5 Summary and outlook

In this work we have used Monte Carlo simulations to study the F model with DWBCs. Although a closed form for the partition function is analytically known for all system sizes, in practice it is particularly useful for the exact computation of certain observables for fairly small systems and to obtain the asymptotic form and its finite-size corrections. Simulations allow for the investigation of systems of moderate size to complement such analytic results as well as to study properties that are not (yet) understood from an analytic point of view.

We have given best estimates for the parameters in the first three subleading finite-size corrections to the energy derived from the asymptotic partition function in Eq. (4.5) at the critical point by fits to the average energies obtained from simulations. This tests the reliability of our simulations; they are precise enough to distinguish the different subleading corrections (Fig. 4.4). The best estimates for the parameters suggest that the first subleading correction is non-negligible in comparison to the leading correction even for macroscopically sized systems, with $L \sim 10^{21}$. We find $\alpha = 1.91 \pm 0.39$ for a previously unknown parameter in the asymptotic expression (4.5) of the domain-wall partition function in the disordered regime found by Bleher and Fokin [129].

Following joint work with Duine and Barkema [3] we have further investigated the order parameter based on the staggered polarization P_0, of which we gave a description in the framework of the quantum-inverse scattering method (QISM). From a theoretical point of view it would be interesting to explore whether it is possible to adapt Baxter's work [108] to obtain an exact expression for P_0 in the case of domain walls, at least in the thermodynamic limit, but we have not done so in the present work. If P_0 is a true order parameter for the model's IOPT, i.e., it is constant on one side of the critical temperature and smoothly starts to change at the phase transition, then the observable $d \ln P_0/d\beta$ must by definition have a divergence at the critical point for infinitely large systems. Using finite-size scaling, and extrapolating to the asymptotic case we have found that $d \ln P_0/d\beta$ does indeed converge to a delta-distribution (see Fig. 4.6), although it fails to give an accurate estimate for the (analytically known) temperature at which the phase transition occurs. Of course the DWBCs together with the ice rule make the system that we have investigated rather special; the observable proposed in Ref. [3] may still be useful for the investigation of other models exhibiting an IOPT. One could also try using the susceptibility of P_0 instead; most of its peaks

lie outside our simulation range, though the peaks that are visible appear to have a comparable quality for finite-size scaling.

In addition to these global (spatially averaged) properties we have studied local properties of the system. The profiles of the c-vertex density $\rho(c)$ obtained for systems of size $L = 512$ at various temperatures with $\Delta \leq 1/2$ are shown in Fig. 4.7. In the antiferroelectric (AF) phase our simulations corroborate the coexistence of three spatially separated phases as found in Refs. [113, 133], with a flat central region exhibiting frozen AF order surrounded by a disordered (D) 'temperate' region and ferroelectrically (FE) ordered corners. Our data agree very well with the arctic curves conjectured by Colomo and Pronko [140] and Colomo, Pronko and Zinn-Justin [141]. It would be desirable to have similar analytic expressions for the 'antartic curve' separating the temperate and AF-frozen regions for $\Delta < -1$.

Regarding the structure inside the temperate region our simulations confirm the oscillations first found by Syljuåsen and Zvonarev [133] and recently recovered by Lyberg *et al.* [135]. Our findings agree with those works, reproducing the patterns visible there, and uncover interesting additional features. Each vertex density oscillates with the same dependence of the wavelength on the position along the diagonal (Fig. 4.8). Our data confirm the conjecture of [133], in accordance with Ref. [135], that these oscillations are finite-size effects: their wavelengths appear to grow sublinearly — roughly as $(0.67 \pm 0.06)L^{(0.553\pm0.016)}$ — and their average amplitudes decrease with system size (Fig. 4.9). Our most detailed result regarding the structure of the temperate region are Figs. 4.10 and 4.11. Here we have chosen to focus on the density difference for the c-vertices since $\rho(c_\pm)$ are in anti-phase (cf. Fig. 4.8), so $\delta\rho(c) := \rho(c_-) - \rho(c_+)$ allows us to study the deviation of one type of vertex around its 'average' without having to know an expression for the latter. We find several types of oscillations. The 'AF' oscillations close to the AF-frozen region appear to be made up of chequerboards of $c_\pm$-vertices that (unlike the AF region in case of even L) survive thermal averaging for even as well as odd L, and are opposite between neighbouring oscillations. The 'FE' oscillations near the FE-frozen region are dominated by the vertices constituting that frozen region; between these oscillations there is a surplus of the type of c-vertices favoured by the DWBCs. In addition there appear to be weak 'higher-order' oscillations in $c_\pm$-densities, forming various saddle-point-like patterns. The oscillations seem to grow weaker as Δ increases. Nevertheless the oscillations persist well into the D phase, with FE and AF oscillations remaining partially visible at $\Delta = 1/2$ (Fig. 4.11). A more quantitat-

ive understanding of these vertex-density oscillations and arrow correlations in the temperate region is desirable, both via simulations and through the analytic methods of Refs. [137, 138], [142], or [123]. In fact, similar finite-size oscillatory behaviour is known to occur for the eigenvalue distributions in random-matrix models[9], see e.g. [154]; this might shed light on the oscillations at least for $\Delta = 0$, cf. [137, 138].

In the near future we plan to report on phase coexistence, arctic-curve phenomena and the structure of the D region for various other choices of boundary conditions; cf. Ref. [148]. Another interesting direction is the study the case of quantum-integrable 'solid-on-solid' (SOS) models, with weights associated to the dynamical Yang–Baxter equation. The trigonometric SOS model is a one-parameter extension of the six-vertex model, and it would be interesting to understand the dependence of those phenomena on the additional 'dynamical' or 'height' parameter. It would also be very exciting if the theoretical and numerical investigations of the F model with domain walls would be complemented by experimental work as in, e.g., Ref. [143].

A Relating configurations with opposite chequerboards in the AF region

In this appendix we show that the F model has symmetries that can be used to sample the whole of phase space starting from any initial configuration obeying the ice rule and DWBCs. We should emphasize that the symmetries we have in mind are symmetries of the model, not of the individual configurations.

We start locally, with the symmetries of the F model at the level of individual vertices shown in Fig. 3.1. Such local symmetries must certainly preserve the lattice near the vertex, i.e. the vertex with its four surrounding edges, so we are led to the dihedral group D_4 of symmetries of the square. Concretely it contains rotations over multiples of $\pi/2$ as well as reflections in the horizontal, vertical and (anti)diagonal line through the vertex. These operations clearly preserve the ice rule. In fact, when the edges carry arrows there is one more thing we can do that is compatible with the ice rule: reversing all arrows, yielding an action of $\mathbb{Z}_2$ that commutes with the D_4.

One can check the preceding operations change the vertex weights as

[9] We thank K. Johansson for pointing this out to us.

follows:

$$\begin{aligned}
\text{reflect } \updownarrow: &\quad a_\pm \leftrightarrow b_\pm\,, \\
\text{reflect } \leftrightarrow: &\quad a_\pm \leftrightarrow b_\mp\,, \\
\text{reflect } \nearrow\!\!\swarrow: &\quad a_+ \leftrightarrow a_-\,, \quad c_+ \leftrightarrow c_-\,, \\
\text{reflect } \nwarrow\!\!\searrow: &\quad b_+ \leftrightarrow b_-\,, \quad c_+ \leftrightarrow c_-\,, \\
\text{rotate } \curvearrowleft: &\quad a_\pm \mapsto b_\mp\,, \quad b_\pm \mapsto a_\pm\,, \quad c_+ \leftrightarrow c_-\,, \\
\text{reverse arrows}: &\quad a_+ \leftrightarrow a_-\,, \quad b_+ \leftrightarrow b_-\,, \quad c_+ \leftrightarrow c_-\,,
\end{aligned}$$

where for each reflection we omit the two weights it preserves. Notice that, when using arrows along the edges to represent the microscopic degrees of freedom, the F model may be characterized as the special case of the six-vertex model for which the vertex weights are invariant under rotations over $\pi/2$, and that they are then further invariant under all of $D_4 \times \mathbb{Z}_2$.

At the global level $D_4 \times \mathbb{Z}_2$ acts on the configurations, where D_4 acts by symmetries of the $L \times L$ lattice if we would forget about the arrows. Not all of these global maps are allowed, though. Regarding the operations corresponding to D_4 the DWBCs are only preserved by a subgroup isomorphic to $\mathbb{Z}_2 \times \mathbb{Z}_2$ corresponding to rotation over π and reflection in the horizontal and vertical symmetry axes of the lattice. However, that the remaining operations in D_4 also preserve the DWBCs if we combine them with arrow reversal[10].

The next question is how these operations act at the level of configurations. Recall that there are two AF ground states, with opposite chequerboard patterns for the alternating c_+- and c_--vertices constituting the AF region; let us call them '0' and '1'. Below the critical temperature ($\Delta < -1$) any configuration is closer (more similar) to one of these two ground states. Accordingly, the phase space decomposes into two parts, say $\mathcal{C}_i$, with $i \in \mathcal{C}_i$ for $i = 0, 1$. For sufficiently low temperatures (or Δ) and large enough L it costs a macroscopically large amount of energy to go from the energetically favourable part of $\mathcal{C}_0$, i.e. configurations close enough to 0, to the corresponding part of $\mathcal{C}_1$: the system is practically trapped in one of these parts. Since we start our Monte-Carlo algorithm from one of the two AF ground states we thus

[10] Thus the full global symmetry group of the F model with DWBCs is a subgroup of $D_4 \times \mathbb{Z}_2$ isomorphic to D_4. Recall that D_4 has a presentation in terms of two generators, r and s, subject to the relations $r^4 = s^2 = (s\,r)^2 = e$. Concretely, r acts by a rotation over $\pi/2$ while s acts by a reflection. Write g^* for the combination of $g \in D_4$ with arrow reversal. Then the subgroup of global symmetries is generated by r^* and s, where the latter acts by reflection in the horizontal or vertical axes; clearly $(r^*)^4 = s^2 = (s\,r^*)^2 = e$. See also (4.18).

expect to stay in the corresponding part of the phase space as the system thermalizes for $\Delta < -1$ and large enough L.

Now we return to the model's symmetries. Consider the two AF ground states, 0 and 1. When L is even the four axes of reflection symmetry meet in the middle of the central face of the lattice, and it follows that the model's symmetries fall into two classes:

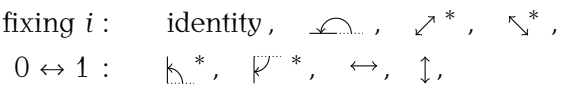

(4.18)

where '*' means combination with arrow reversal. More generally, (4.18) indicates how the model's global symmetries relate the $\mathcal{C}_i$.

Since for the F model these operations do not change the vertex weights, they preserve the energy of the configurations. Given any configuration we can act by the model's symmetries to generate further configurations of the same energy; we get up to eight configurations in this way, though it may be only four or two if the original configuration happened to possess some amount of symmetry. (One should really check for such symmetries of the original configuration to avoid overcounting, but at high enough L we can skip this step as such symmetric configurations make up a negligible portion of the phase space.) Half of the configurations we get in this way lie in $\mathcal{C}_0$ and the other half in $\mathcal{C}_1$. The upshot is that after having run the Monte Carlo simulation we can use the model's symmetries to sample the full phase space, even from simulations that correctly sample around one of the two ground states.